

# A General Method for Estimation of Fracture Surface Roughness: Part II. Practical Considerations

A.M. GOKHALE and W.J. DRURY

Surface roughness is an important attribute of fracture surfaces. An assumption-free method for estimation of surface roughness presented in Part I<sup>[1]</sup> is analyzed further here. It is shown that three vertical sectioning plane orientations mutually at an angle of 120 deg contain sufficient information for a reliable estimation of surface roughness; in most of the cases, the sampling error due to measurements on a limited number (three) of vertical section orientations should be less than  $\pm 6$  pct with a confidence limit of 95 pct. A simplified procedure is presented for calculation of a profile structure factor from the measurements of the profile frequency function. A practical example of application of the present analysis involving measurement of the fracture surface roughness of a metal-matrix composite is discussed.

## I. INTRODUCTION

THE surface roughness parameter is a quantitative index of fracture surface roughness. The nature of fracture surface and its roughness depend on the material chemistry, microstructure, and the deformation and fracture process that lead to fracture. In Part I,<sup>[1]</sup> a general theoretical treatment has been presented for the estimation of the fracture surface roughness parameter,  $R_S$ , from the measurements performed on the vertical section fracture profiles. Such fracture profiles are lines (usually of irregular shape) generated by intersections of the fracture surface with the metallographic sectioning planes perpendicular to the average topographic plane of the fracture surface. Thus, all of the vertical sectioning planes contain the direction normal to the average topographic plane of the fracture surface; this common direction or "zone axis" is called the "vertical axis." The estimation of the fracture surface roughness parameter,  $R_S$ , involves the following measurements on the vertical section fracture profiles.

- (1) the fracture profile roughness parameter,  $R_L$ , which is equal to the true length of the fracture profile divided by its apparent projected length (overlaps not counted) on a line perpendicular to the vertical axis and in the corresponding vertical sectioning plane<sup>[2]</sup> (Figure 1), and
- (2) the profile structure factor,  $\psi$ , defined as follows:<sup>[1]</sup>

$$\psi \equiv \int_0^\pi \sin \theta \int_0^\pi |\cos(\theta + \pi/2 - \alpha)| \cdot f(\alpha) d\alpha d\theta \quad [1]$$

where  $\alpha$  is the angle between the tangent to an arc element on the fracture profile and the vertical axis (Figure 1); it specifies the angular orientation of an arc element. In general, different line or arc elements on a fracture profile have different angular orientations;  $f(\alpha)$  is the frequency distribution function of arc element orientations in the fracture profile. Thus,  $f(\alpha) d\alpha$  is equal to the frac-

tion of profile length in the orientation range  $\alpha$  to  $(\alpha + d\alpha)$ . For the present purpose,  $\theta$  is simply a dummy variable of integration in Eq. [1]. Thus,  $\psi$  is completely determined by  $f(\alpha)$ .

The parameters  $R_L$  and  $\psi$  can be experimentally measured. In general, vertical sectioning planes of different angular orientations may result in fracture profiles having different values of  $R_L$  and  $\psi$ . It can be shown that<sup>[1]</sup>

$$R_S = \overline{R_L \cdot \psi} \quad [2]$$

where  $\overline{R_L \cdot \psi}$  is an expected or average value of the product of  $R_L$  and  $\psi$  on a set of vertical sectioning planes. Note that an average value of the product of  $R_L$  and  $\psi$ , and *not* the product of the average values of  $R_L$  and  $\psi$ , is the quantity equal to  $R_S$ . Equation [2] is absolutely general, and it does not involve any assumptions concerning the nature of the fracture surface. This result forms the basis for an assumption-free and unbiased estimation of the fracture surface roughness parameter,  $R_S$ , from the measurements of  $R_L$  and  $\psi$  performed on the vertical section fracture profiles.

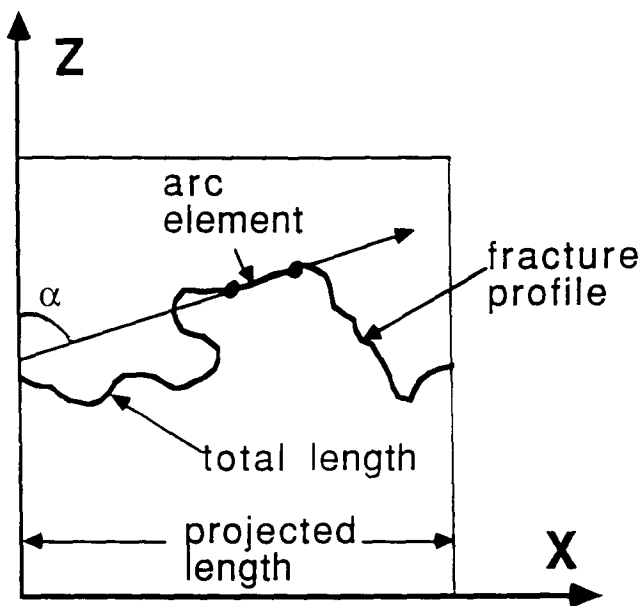
It is the purpose of this paper to focus on the practical aspects associated with application of Eq. [2] for estimation of fracture surface roughness. The estimation of  $R_S$  involves measurements of  $R_L$  and  $\psi$  on a number of vertical sectioning planes of different angular orientations. This amounts to statistical sampling of  $R_L\psi$  values from the population, which raises two questions of significant practical importance:

- (1) On how many vertical sectioning plane orientations is it necessary to measure  $R_L$  and  $\psi$  to obtain a reliable estimate of  $\overline{R_L\psi}$  and, hence,  $R_S$ ?
- (2) How close (or how reliable) is the *sample* average  $(\overline{R_L\psi})_s$  to the population average  $\overline{R_L\psi}$ , i.e.,  $R_S$ ?

This sampling problem is analyzed in Section II with the aid of computer simulations. It is shown that the measurements on three vertical sectioning plane orientations mutually at an angle of 120 deg are sufficient for a reliable estimation of  $R_S$ . In the subsequent section, a simple procedure is presented for analytical as well as numerical calculation of the profile structure factor,  $\psi$ . Finally, a practical example of an estimation of  $R_S$  is given for the fracture surface of a metal-matrix composite.

A.M. GOKHALE, Associate Professor, and W.J. DRURY, Graduate Research Assistant, are with the School of Materials Engineering, Georgia Institute of Technology, Atlanta, GA 30332-0245.

Manuscript submitted August 28, 1989.



$$R_L = \frac{\text{profile length}}{\text{projected length}}$$

Fig. 1—Definition of  $R_L$  and profile element orientation angle,  $\alpha$ .

## II. EFFICIENT SAMPLING PROCEDURE

Angular orientation of a surface element  $\delta S$  on a fracture surface is given by angles  $\theta_s$  and  $\phi_s$  pertaining to its normal  $\mathbf{N}_s$ , as shown in Figure 2. Note that the  $z$ -axis is the vertical axis (direction perpendicular to the average topographic plane of the fracture surface),  $\theta_s$  is the angle between the normal  $\mathbf{N}_s$  and  $z$ -axis, and  $\phi_s$  is the angle between the projection of  $\mathbf{N}_s$  on the  $xy$  plane and  $x$ -axis. The choice of the  $x$ -axis is arbitrary in the plane perpendicular to the  $z$ -axis. In general, different surface elements on a fracture surface may have different angular orientations. Let  $g(\phi_s, \theta_s)$  be the angular orientation distribution function (SODF) of the surface elements on a fracture surface, such that  $g(\phi_s, \theta_s) \sin \theta_s d\phi_s d\theta_s$  is equal to the fraction of fracture surface area having angular orientations in the range of  $\phi_s$  to  $(\phi_s + d\phi_s)$  and  $\theta_s$  to  $(\theta_s + d\theta_s)$ . The SODF  $g(\phi_s, \theta_s)$  quantifies the fracture surface anisotropy. Intersection of a surface element,  $\delta S$ , on the fracture surface with a vertical sectioning plane yields an arc element,  $d\lambda$ , on the vertical section fracture profile. The length of such an arc element and its angular orientation,  $\alpha$ , in the sectioning plane (Figure 1) basically depend on the orientation of the surface element,  $\delta S$ , given by angles  $\phi_s$  and  $\theta_s$  and the orientation of the vertical sectioning plane given by the angle  $\phi_p$  (Figure 3). It follows that changes in  $f(\alpha)$ , and hence  $\psi$ , with the variations in the vertical sectioning plane orientation,  $\phi_p$ , are basically determined by the SODF  $g(\phi_s, \theta_s)$ . Similarly, the SODF also determines variations of  $R_L$  as a function of the sectioning plane orientation,  $\phi_p$ . In other words, the range of values of the product  $R_L\psi$  (or "spread" around the mean) in a population of vertical section fracture profiles of a given frac-

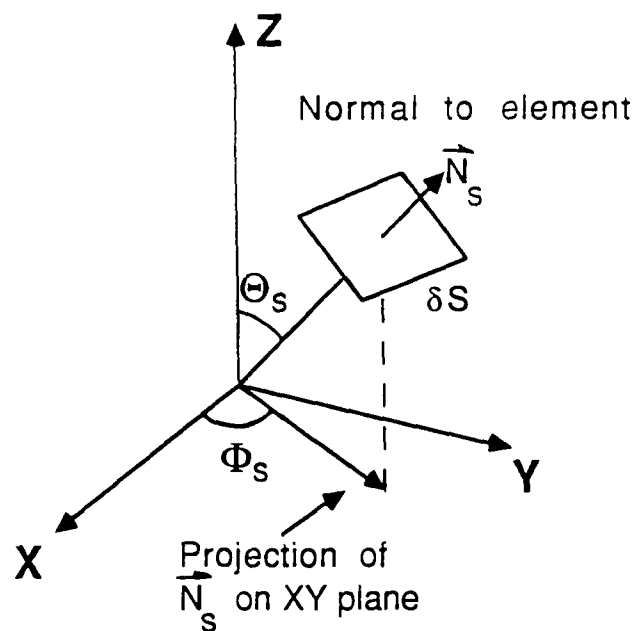


Fig. 2—Angular orientation of a surface element.

ture surface is determined by the SODF  $g(\phi_s, \theta_s)$ . Thus, the average of population of  $R_L\psi$  values is always equal to  $R_S$ , but the *variance* is determined by the SODF of the fracture surface under investigation. Usually, the SODF  $g(\phi_s, \theta_s)$  is unknown. For a randomly oriented fracture surface,  $g(\phi_s, \theta_s)$  is constant (*i.e.*, all of the orientations are equally likely); hence, all of the fracture profiles are statistically similar, and measurements on a

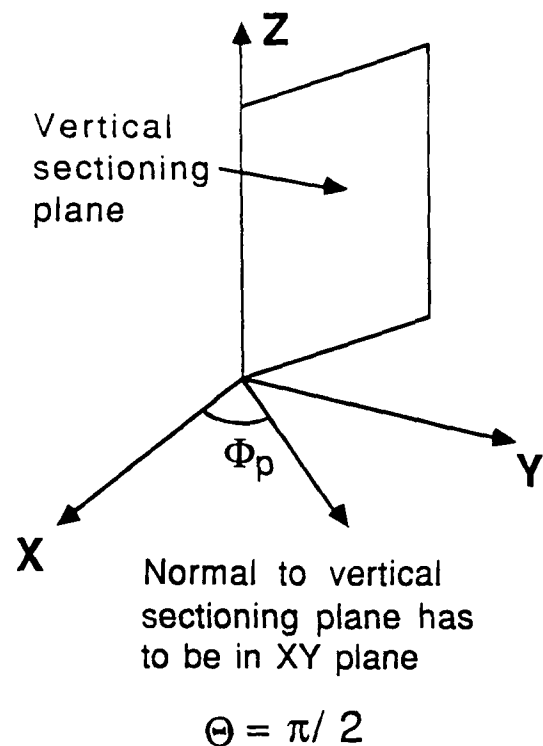


Fig. 3—Orientation of a vertical sectioning plane.

single vertical section orientation can yield a reliable estimate of  $R_S$ . However, real fracture surfaces are unlikely to be randomly oriented due to the basic nature of the fracture processes. If the SODF depends only on  $\theta_S$  and *not* on  $\phi_S$  [*i.e.*,  $g(\phi_S, \theta_S) = g(\theta_S)$ ], then the SODF is symmetric with respect to the vertical axis; *i.e.*, for any given interval  $\theta_S$  and  $(\theta_S + d\theta_S)$ , all of the  $\phi_S$  angles are equally likely. In such a case, all of the vertical section fracture profiles are statistically similar, and variance of  $R_L\psi$  values is expected to be very small. Hence, measurement of  $R_L\psi$  on a single vertical section orientation should give a reliable estimate of  $R_S$ . If the SODF depends on both  $\theta_S$  and  $\phi_S$ , then different vertical section orientations can yield different values of  $R_L\psi$ . The range of values of  $R_L\psi$  in a population of vertical sections thus depends on how sensitive the SODF  $g(\phi_S, \theta_S)$  is to the orientation parameter,  $\phi_S$ . The limiting case is a surface where all of the surface elements have the same value of  $\phi_S$  (although they may have different  $\theta_S$  values); *i.e.*,

$$g(\phi_S, \theta_S) = \delta(\phi_S^1) \cdot g(\theta_S) \quad [3]$$

where  $\delta(\phi_S^1)$  is a delta function around  $\phi_S = \phi_S^1$ , and  $g(\theta_S)$  is a function of  $\theta_S$  only. The surfaces whose SODFs can be represented by Eq. [3] thus exhibit large variations in  $R_L\psi$  values in the vertical section fracture profiles. It follows that such surfaces would require measurements of  $R_L$  and  $\psi$  on a number of vertical section orientations to obtain a reliable value of  $R_L\psi$  and, hence,  $R_S$ . It follows that the number of vertical section orientations necessary to obtain a reliable  $R_S$  value of such surfaces should be sufficient for a reliable estimation of the fracture surface roughness of *any* fracture surface. Thus, the problem reduces to determination of the number of vertical sectioning plane orientations necessary for a reliable estimation of  $R_S$  of the surfaces whose SODFs have functional form given by Eq. [3] and the development of an efficient sampling scheme to minimize the sampling error. A class of "ruled surfaces" of geometry<sup>[3]</sup> has the required form of SODF. Such ruled surfaces can be generated by moving a planar curve in a direction perpendicular to the plane of the curve. Figure 4 gives three examples of ruled surfaces and the corresponding generating planar curves. A corrugated sheet is an example of a ruled surface. In Figure 5, the normal vector of any surface element is parallel to the  $yz$  plane; hence, the  $\phi_S$  orientation angle of all of the surface elements is equal to  $\pi/2$ . Thus, the SODF of such ruled surfaces can be represented by Eq. [3] with  $\phi_S^1$  equal to  $\pi/2$ ; the function  $g(\theta_S)$  is obviously determined by the nature of the generating planar curve. These ruled surfaces have the following properties:<sup>[4]</sup>

- (1)  $R_L$  is always equal to 1.0 on the vertical section perpendicular to the planar curve and
- (2)  $R_L$  has a maximum value  $(R_L)_m$  on the vertical section which contains the planar generating curve, and  $(R_L)_m$  is precisely equal to the  $R_S$  of the ruled surface.

In the present study, a ruled surface having a "semi-circular wave" generating curve (Figure 4(a)) was simulated on the CYBER\* 760 mainframe computer at

\*CYBER is a trademark of Control Data Corporation, Minneapolis, MN.

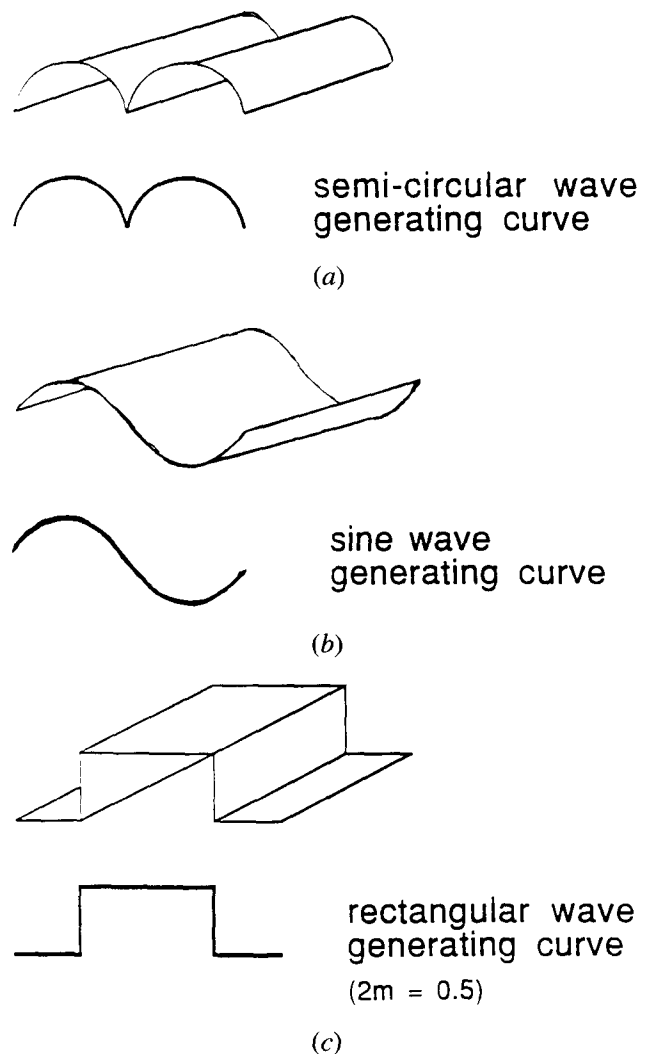


Fig. 4—Examples of ruled surfaces: (a) ruled surface with semi-circular wave generating curve; (b) ruled surface having sine wave generating curve; and (c) ruled surface having rectangular wave generating curve.

Georgia Institute of Technology. It is assumed that the surface is of infinite extent and, hence, there are no "edge effects." The surface was sectioned by vertical sectioning planes of different orientations  $\phi_p$  at intervals of 1 deg in the range of 0 to 180 deg. The values of  $R_L$  and  $\psi$  on

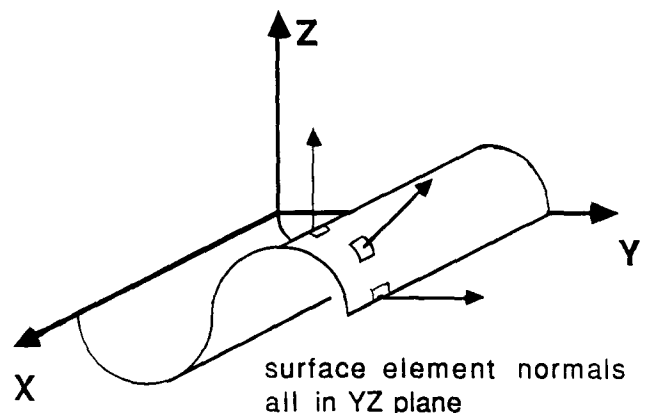


Fig. 5—Orientations of surface elements on a ruled surface.

resulting vertical section profiles were calculated and stored in the computer memory. Next, three random number integers in the interval of 0 to 180 were computer-generated independently, each number representing a vertical section orientation. The average of the  $R_L\psi$  values of these three independent random vertical section profiles was calculated. Let this sample average be  $(\overline{R_L\psi})_S$ . The process was repeated 1000 times, each simulation representing vertical section sampling by three planes of independent random orientations. Figure 6 reports the frequency of occurrence of the sample average,  $(\overline{R_L\psi})_S$ , in the 1000 simulations. Inspection of Figure 6 shows that

- (1) the expected value of  $(\overline{R_L\psi})_S$  is indeed equal to  $R_S$  and
- (2) there is a very large spread in the  $(\overline{R_L\psi})_S$  values.

Increasing the number of sections up to seven did not decrease the spread in  $(\overline{R_L\psi})_S$  significantly. It must be concluded that the measurements on independent random vertical sections cannot yield a reliable estimate of  $R_S$  unless the measurements are performed on an extremely large number of vertical section orientations. An alternative to independent random vertical sections is *systematic* vertical section sampling,<sup>[5]</sup> where the first vertical section orientation is random but subsequent orientations are *chosen* with respect to the first one in a systematic manner. This was carried out as follows:

- (1) The computer generated a random number integer in the interval of 0 to 180 deg, representing the orientation of the *first* vertical section  $\phi_p^R$ .
- (2) Orientations of second and third vertical sections were *fixed* at  $(\phi_p^R + 120 \text{ deg})$  and  $(\phi_p^R + 240 \text{ deg})$ , respectively. The average value of  $R_L\psi$  of the corresponding three vertical section profiles,  $(\overline{R_L\psi})_{SS}$ , was calculated.
- (3) Steps (1) and (2) were repeated 1000 times, representing 1000 experiments consisting of sampling by a randomly rotated triplet of three sectioning planes mutually at an angle of 120 deg. Figure 7 reports the frequency of occurrence of  $(\overline{R_L\psi})_{SS}$  values of the systematic samples generated in the 1000 simulations. It is interesting to note that

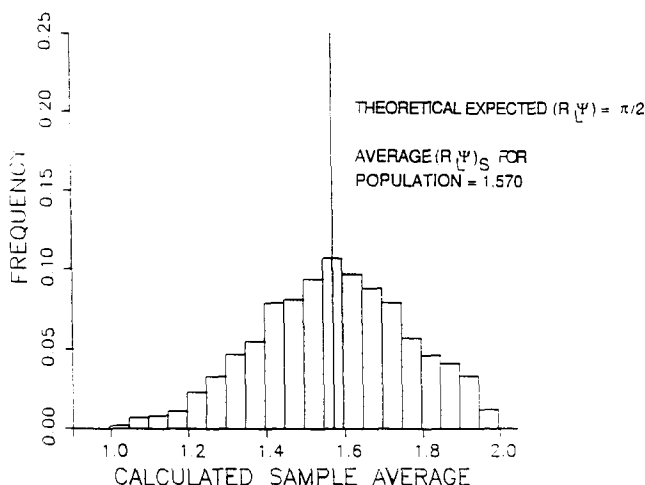


Fig. 6—Frequency of  $(\overline{R_L\psi})_S$  values for three independent random vertical sections; the population average:  $(\overline{R_L\psi})_S = R_S = \pi/2$ .

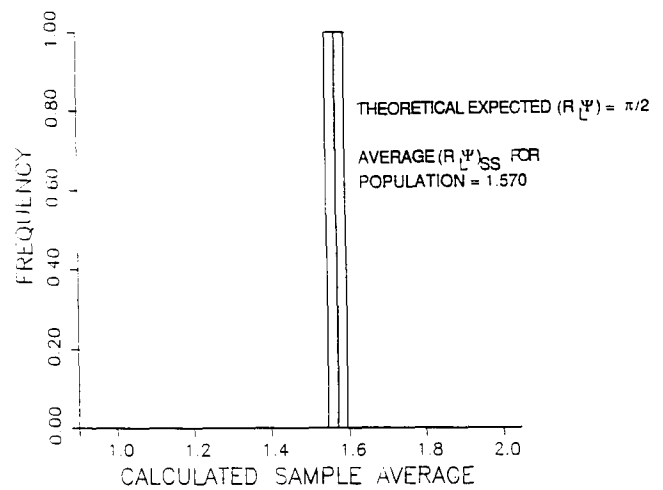


Fig. 7—Frequency of  $(\overline{R_L\psi})_{SS}$  values for systematic sampling by three vertical sections mutually at 120 deg; population average:  $(\overline{R_L\psi})_S = R_S = \pi/2$ .

- (a) the expected value of  $(\overline{R_L\psi})_{SS}$  is equal to  $R_S$  and
- (b) all of the values of  $(\overline{R_L\psi})_{SS}$  lie in a very narrow range of 1.545 to 1.595, *i.e.*,  $1.57 \pm 0.025$ .

Thus, one experiment involving three vertical section orientations mutually at an angle of 120 deg yields values of  $R_S$  with an error of less than  $\pm 2$  pct for a ruled surface having a “semicircular wave” generating curve. In order to determine whether these results are sensitive to the shape of generating planar curve associated with ruled surface (*i.e.*,  $g(\theta_S)$  in Eq. [3]), the following additional ruled surfaces were analyzed:

- (1) a ruled surface with sine wave generating curve (Figure 4(b)) and
- (2) a ruled surface with rectangular wave generating curve (Figure 4(c)).

The ruled surface with sine wave generating curve was simulated on a computer, and systematic vertical section sampling was carried out as discussed earlier. The basic conclusions remain unchanged: a single experiment consisting of three vertical section orientations mutually at 120 deg gives the value of  $(\overline{R_L\psi})_{SS}$  with a sampling error of less than  $\pm 2$  pct. The ruled surface with rectangular generating wave (Figure 4(c)) can be analyzed in a straightforward manner. Using simple geometric arguments, it can be shown that

$$R_S = 1 + 2m \quad [4]$$

$$R_L\psi = 1 + \pi m |\cos \phi_p| \quad [5]$$

where  $R_L\psi$  is the value pertaining to the profile associated with the vertical section having orientation  $\phi_p$  and  $2m$  is equal to the ratio of the total length of the vertical line segments of the rectangular generating curve to the total length of its horizontal line segments. If  $m = 1$ , two-thirds of the *surface* elements have orientation  $\phi_S = \pi/2$ ,  $\theta_S = \pi/2$ . The variation of  $m$  essentially reflects a change in the function  $g(\theta_S)$  in Eq. [3]. If  $m = 2$ , 80 pct of the surface area is parallel to the vertical axis (*i.e.*,

$\phi_s = \pi/2$ ,  $\theta_s = \pi/2$ ), an extreme case of anisotropy. For systematic vertical section sampling consisting of three vertical planes mutually at 120 deg, Eq. [4] yields the following result:

$$R_s = R_L \cdot \psi = 1 + \frac{\pi m}{3} \left[ \left| \cos \phi_p \right| + \left| \cos \left( \phi_p + \frac{2\pi}{3} \right) \right| + \left| \cos \left( \phi_p + \frac{4\pi}{3} \right) \right| \right] \quad [6]$$

where  $\phi_p$  is the orientation of the first vertical section.  $(R_L \psi)_{SS}$  was calculated for different values of  $\phi_p$  at an interval of 1 deg in the range of 0 to 120 deg. It was observed that 95 pct of the  $(R_L \psi)_{SS}$  values were within  $\pm 5$  pct of the  $R_s$  value for ruled surface with  $m = 1$ , and 95 pct of the  $(R_L \psi)_{SS}$  values were within  $\pm 6$  pct of the  $R_s$  value for  $m = 2$ . Note that the  $R_s$  value of a surface with  $m = 2$  is 5.0 (Eq. [5]), and for this surface, 80 pct of the surface area is parallel to the vertical axis. Real fracture surfaces are not generally expected to have surface roughness higher than 5.0, and they are also not expected to exhibit anisotropy worse than that of a rectangular wave ruled surface with  $m = 2$ . It is interesting to note that for a ruled surface with a semicircular wave generating curve,  $g(\theta_s)$  (Eq. [3]) is constant (*i.e.*, line elements on the generating curve have random orientations in the plane of the curve), whereas for a rectangular wave ruled surface,  $g(\theta_s)$  basically consists of two spikes (one at  $\theta_s = 0$  and a second at  $\theta_s = \pi/2$ ). For a sine wave ruled surface,  $g(\theta_s)$  has a complicated form. However, in all three cases, at least 95 pct of  $(R_L \cdot \psi)_{SS}$  values are within  $\pm 6$  pct of the corresponding  $R_s$  value.

The SODF of any arbitrary fracture surface can be written in the following form:

$$g(\theta_s, \phi_s) = g_0(\theta_s) + \sum \delta(\phi_s^i) \cdot g_i(\theta_s) \quad [7]$$

where  $\delta(\phi_s^i)$  are delta functions around different  $\phi_s = (\phi_s^i)$  and  $g_i(\theta_s)$  are functions of  $\theta_s$  only. Thus, the SODF of any fracture surface can be represented by a combination of SODFs of randomly oriented surface, rotationally symmetric surface (*i.e.*,  $g_0(\theta_s)$ ), and a number of ruled surfaces. In all of these three limiting cases, systematic vertical section sampling with three vertical sectioning planes mutually at an angle of 120 deg is sufficient to obtain an  $R_s$  value with an error of less than  $\pm 6$  pct with 95 pct confidence. This sampling should also be sufficient for any arbitrary fracture surface, as it can be regarded as the one resulting from superimposition of a number of different ruled surfaces, a rotationally symmetric surface, and a random surface (see Eq. [7]).

The above analysis leads to the following conclusions applicable to any fracture surface:

- (1) Systematic vertical section sampling is extremely efficient as compared to sampling by independent random vertical sections.
- (2) One experiment consisting of three vertical section orientations mutually at an angle of 120 deg is sufficient to yield an  $R_s$  value with a sampling error of less than  $\pm 6$  pct with a 95 pct confidence limit for real fracture surfaces.

### III. CALCULATION OF PROFILE STRUCTURE FACTOR

The experimental data on profile element orientation angles  $\alpha$  (Figure 1) can be conveniently grouped into histogram form. The values of  $\alpha$  range from 0 to 180 deg; this range can be divided into  $K$  classes having class interval  $\Delta$  (where  $\Delta = \pi/K$ ). Let  $h_i \Delta$  be the fraction of profile length having the orientation angle  $\alpha$  in the range  $(i-1)\Delta$  to  $i\Delta$ . Thus,  $h_i$  is the height of  $i$ th histogram bar, and the index  $i$  takes integer values from 1 to  $K$ . By definition,

$$h_i \Delta = \int_{(i-1)\Delta}^{i\Delta} f(\alpha) d\alpha \quad [8]$$

and,

$$\sum_{i=1}^K h_i \Delta = 1 \quad [9]$$

Equations [1] and [8] lead to the following results:

$$\psi = \int_0^\pi \sin \theta \cdot \Delta \cdot \sum_{i=1}^K \left| \cos \left[ \theta + \frac{\pi}{2} - \left( i - \frac{1}{2} \right) \Delta \right] \right| \cdot h_i \cdot d\theta \quad [10]$$

or

$$\psi = \Delta \cdot \sum_{i=1}^K a_i h_i \quad [11]$$

where

$$a_i = \int_0^\pi \sin \theta \cdot \left| \cos \left[ \theta + \frac{\pi}{2} - \left( i - \frac{1}{2} \right) \Delta \right] \right| \cdot d\theta \quad [12]$$

A simple algebraic manipulation of Eq. [12] gives the following result:

$$a_i = \sin \left[ \left( i - \frac{1}{2} \right) \Delta \right] + \left[ \frac{\pi}{2} - \left( i - \frac{1}{2} \right) \Delta \right] \cdot \cos \left[ \left( i - \frac{1}{2} \right) \Delta \right] \quad [13]$$

The coefficients  $a_i$  depend on  $i$ , but they are independent of the nature of the frequency function (*i.e.*, they do not depend on  $h_i$  values). Thus, the same set of values of the coefficients  $a_i$  can be utilized to calculate the profile structure factor,  $\psi$ , of any fracture profile. Table I reports numerically calculated values of  $a_i$ , in which the data are grouped into 18 histograms of width  $\Delta = \pi/18 = 10$  deg. This table and Eq. [11] provide a straightforward procedure for calculation of  $\psi$ . If it is necessary to group the data into a total number of classes other than 18 (*i.e.*,  $K \neq 18$ ), then Eq. [12] or [13] can be utilized for calculation of  $a_i$  coefficients.

### IV. PRACTICAL EXAMPLE

Figure 8 is a scanning electron microscopy (SEM) fractograph of the fracture surface of a composite material consisting of continuous unidirectional fibers of

**Table I. Calculated Values of  $a_i$  Coefficients**

$i$	$a_i^*$	$i$
1	1.565	18
2	1.5232	17
3	1.4508	16
4	1.3599	15
5	1.2625	14
6	1.1694	13
7	1.0906	12
8	1.0336	11
9	1.0037	10

\*The values are symmetric with respect to  $\alpha = \pi/2$ .

alumina in the matrix of Al-Li alloy. The material was fractured by application of uniaxial tensile stress perpendicular to the fibers. The fracture surface is anisotropic because of the material's anisotropic microstructure. The profile structure factor,  $\psi$ , and the profile roughness parameter,  $R_L$ , are expected to depend on the orientation of the vertical sectioning plane. The steps involved in the estimation of  $R_S$  are as follows:

- (1) Thick plating of fracture surface ( $\cong 25 \mu\text{m}$ ) to avoid distortion during sectioning and metallographic polishing. In the present case, the specimen was electroplated with a thick layer of copper.
- (2) Metallographic sectioning along three vertical sectioning planes mutually at an angle of 120 deg and subsequent metallographic polishing using standard techniques to clearly reveal the fracture profiles. Figures 9 through 11 show the fracture profiles obtained in this manner.
- (3) Digitization of fracture profiles *via* semiautomatic or automatic digital image analysis. In the present case, the profiles were digitized using a Zeiss digitizing tablet attached to a Video-Plan semiautomatic image analyzer. The process involves manual tracing of the fracture profile using an electronic cursor. The instrument records the coordinates of points on the fracture profile at pre-selected fixed intervals; the interval length is called "ruler length." The profile is thus represented by a series of line segments (Figure 12); the total profile length,  $\lambda_0$ , is

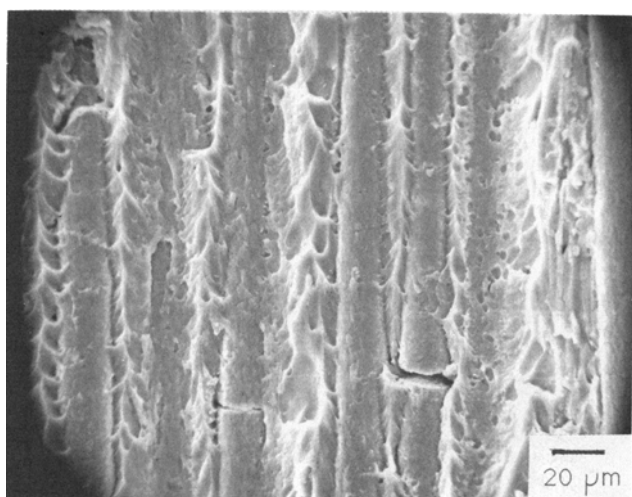


Fig. 8—SEM fractograph of fracture surface of a metal-matrix composite.

$\Phi = 0$  degrees

$R_L = 2.16$

$\Psi = 1.27$

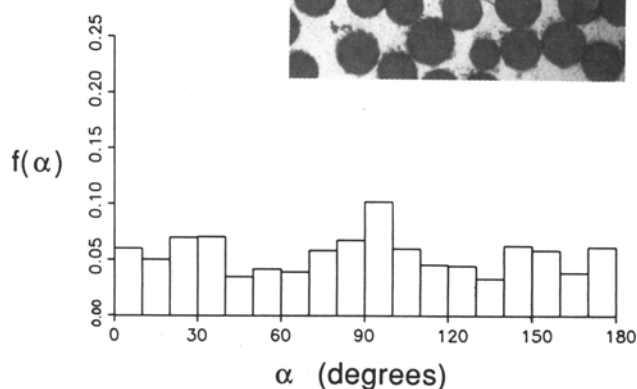


Fig. 9—Vertical section fracture profile ( $\phi = 0$  deg) and corresponding profile frequency function,  $f(\alpha)$ .

equal to the sum of the lengths of all the line segments. The instrument also measures the angle  $\alpha$  between each digitized line segment and the vertical axis. The frequency of these  $\alpha$  values is the profile frequency function  $f(\alpha)$ . The values of  $R_L$  and  $f(\alpha)$  were obtained in this manner and are reported in Figures 9 through 11.

(4) The profile structure factor,  $\psi$ , is calculated by substituting histogram bar heights,  $h_i$ , and  $a_i$  values from Table I in Eq. [11].

(5) The fracture surface roughness parameter,  $R_S$ , is equal to the average value of the product,  $R_L\psi$ , on the three vertical sections. In the present case,  $R_S$  is estimated to be equal to 2.17.

## V. DISCUSSION

It is shown that<sup>[1]</sup> the fracture surface roughness parameter,  $R_S$ , can be estimated from the measurements of

$\Phi = 120$  degrees

$R_L = 1.61$

$\Psi = 1.20$

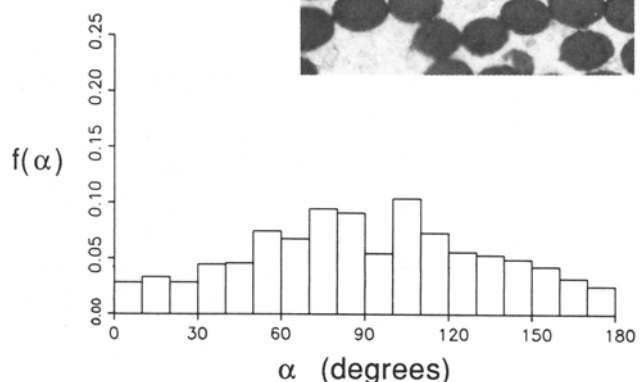


Fig. 10—Vertical section fracture profile ( $\phi_p = 120$  deg) and corresponding profile frequency function,  $f(\alpha)$ .

$\Phi = 240$  degrees

$R_L = 1.54$

$\Psi = 1.19$

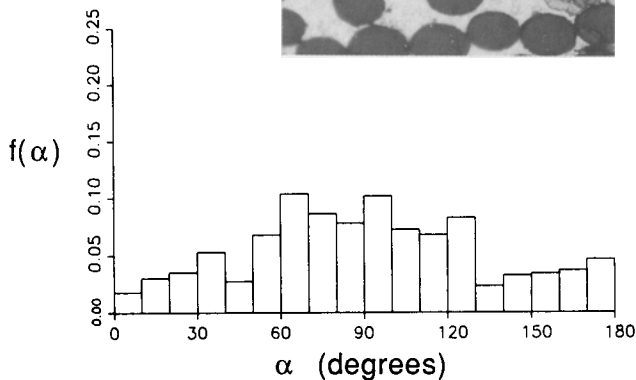
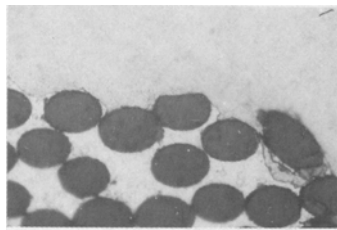


Fig. 11—Vertical section fracture profile ( $\phi_p = 240$  deg) and corresponding profile frequency function,  $f(\alpha)$ .

the profile roughness parameter,  $R_L$ , and the profile structure factor,  $\psi$ , on the vertical section fracture profiles; measurements on three vertical section angular orientations mutually at an angle of 120 deg can yield a reliable estimate of  $R_S$ . It is often observed that  $R_L$  varies systematically with the resolution or the “ruler length” utilized for profile digitization. Careful experimental work of Underwood and Banerji<sup>[6]</sup> demonstrated that although  $R_L$  increases with the decrease in the ruler length,  $\eta$ , it approaches a finite value  $(R_L)_0$  as  $\eta \rightarrow 0$ . In other words,  $R_L$  does not approach  $\infty$  as  $\eta \rightarrow 0$ , and hence, fracture profiles do not exhibit the classical fractal characteristics proposed by Mandelbrot.<sup>[7]</sup> The present analysis is applicable to the  $R_L$  value measured at any length of the ruler,  $\eta$ ; the estimated  $R_S$  value reflects surface roughness at a similar level of resolution. The analysis is equally applicable to the extrapolated “true” profile roughness value  $(R_L)_0$  as  $\eta \rightarrow 0$ ; the estimated value of  $R_S$  then represents the surface roughness corresponding to  $\eta^2 \rightarrow 0$ .

The metallographic sectioning of fracture surface by vertical sectioning planes is proposed in the present work. However, actual physical sectioning of fracture surfaces is not necessary for application of the present analysis. For example, stereo pair images<sup>[8]</sup> can be utilized to gen-

erate the coordinates of points on a fracture surface along different directions using SEM, and the present procedure can then be utilized for estimation of  $R_S$ ; this is expected to be more efficient as compared to generation of a “carpet plot” of fracture surface, because it involves sampling of the surface along *lines* rather than *areas*.

It is likely that the surface roughness parameter,  $R_S$ , may correlate to the fracture toughness of materials. However, to develop such correlations, it is necessary to estimate  $R_S$  without invoking any assumptions concerning the nature of the fracture surface (which can be done using the present procedure). On the other hand, the profile roughness parameter,  $R_L$ , may not correlate to fracture toughness or any other fracture process descriptors for the simple reason that two or more surfaces with different  $R_S$  values can yield fracture profiles having the same value of  $R_L$ ! Finally, it must be pointed out that surface roughness is only one geometric attribute of a given fracture surface. Thus, two fracture surfaces having the same value of  $R_S$  need not be similar. A detailed characterization of fracture surface geometry should be possible *via* estimation of the orientation distribution function  $g(\phi_s, \theta_s)$  and  $R_S$ . Unfortunately, at present, there is no general, practically feasible procedure for estimation of the orientation distribution function from measurements performed on fracture profiles.

## VI. CONCLUSIONS

An efficient sampling procedure is proposed for estimation of fracture surface roughness from the measurements performed on the vertical section fracture profiles. It is shown that appropriate measurements performed on three vertical section orientations mutually at 120 deg yield reliable estimates of the surface roughness parameter,  $R_S$ .

## ACKNOWLEDGMENT

This research work is part of a National Science Foundation sponsored project (DMR-8504167) on “Quantitative Analysis of Fracture Surfaces Using Stereological Methods;” this financial support is gratefully acknowledged.

## REFERENCES

1. A.M. Gokhale and E.E. Underwood: *Metall. Trans. A*, 1990, vol. 21A, pp. 1193-99.
2. J.P. Pickens and J. Gurland: *Proc. 4th Int. Congr. for Stereology*, E.E. Underwood, R. deWit, and G.A. Moore, eds., NBS Spec. Publ. 431, Gaithersburg, MD, 1976, pp. 269-72.
3. D.J. Struik: *Classical Differential Geometry*, 2nd ed., Addison-Wesley Publishing Co., Reading, MA, 1961, pp. 62-72.
4. E.E. Underwood and K. Banerji: *ASM Metals Handbook*, 9th ed., ASM, Metals Park, OH, 1987, vol. 12, pp. 189 and 192-210.
5. H.J.G. Gundersen and E.B. Jensen: *J. Microsc.*, 1987, vol. 147, pp. 229-63.
6. E.E. Underwood and K. Banerji: *ASM Metals Handbook*, 9th ed., ASM, Metals Park, OH, 1987, vol. 12, pp. 211-15.
7. B.B. Mandelbrot: *The Fractal Geometry of Nature*, W.H. Freeman and Company, New York, NY, 1982.
8. L.S. Sigl and H.E. Exner: *Metall. Trans. A*, 1987, vol. 18A, pp. 1299-1308.

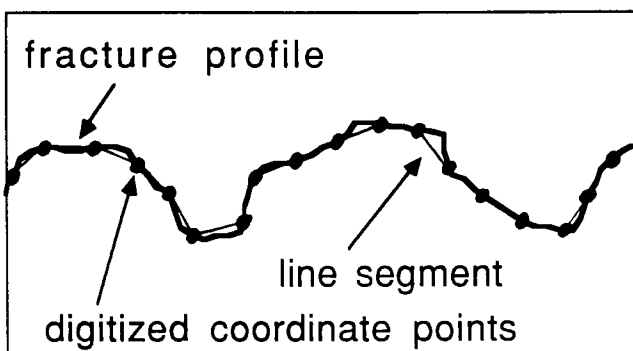


Fig. 12—Digitization of fracture profile.